

Novel Applications of Secondary Ion Mass Spectrometry in Optoelectronic Materials Studies*

Steven A. Schwarz

Bellcore, Red Bank, NJ 07701-7040, USA

Received July 12, 1993

Several optoelectronic material studies which exploit the high sensitivity and high depth resolution of the SIMS (secondary ion mass spectrometry) technique, all employing a quadrupole SIMS instrument located at the author's institution, are reviewed. Solid phase Pd/Ge and Pd/Si based contacts on GaAs and InP are examined by "backside SIMS." In this technique, the semiconductor substrate is etched away while preserving a 300 nm epitaxial marker layer structure on which the contact resides. Depth resolution is greatly enhanced by sputter profiling through the thin semiconductor layer into the metallic region. In the Pd/Ge/GaAs ohmic contact, the Ge dopant profile is observed to drop by 4 orders of magnitude within ~ 10 nm of the metal/GaAs interface. Solid phase III-V regrowth is detected in both the GaAs and InP Pd/Ge contacts. Backside SIMS is also employed in an examination of low energy channeling of Si into GaAs. SIMS studies of dopant induced interdiffusion in GaAs/AlGaAs and InP/InGaAs superlattices exploit the sensitivity of SIMS to minute changes in stoichiometry. Measurements of diffusion length as a function of dopant concentration and temperature provide strong support for the prediction that cation diffusion is mediated by the triply charged Ga vacancy in GaAs. A study of interdiffusion induced strain in the InP/InGaAs system reveal the importance of partial dislocation pairs for strain relaxation. The sensitivity of SIMS to small changes in sample stoichiometry is exploited in studies of Ga reevaporation and growth feedback control during molecular beam epitaxy (MBE) growth of AlGaAs. Studies of segregation and ordering in polymer blends are briefly described.

I. Introduction

Secondary ion mass spectrometry (SIMS) is a high depth resolution (~ 10 nm) high sensitivity (often less than 1 part per million) technique frequently employed in the characterization of optoelectronic materials. The recent acquisition of two sophisticated quadrupole SIMS instruments in the state of São Paulo, Brazil motivates this review of novel SIMS applications on the occasion of the 6th Brazilian School on Semiconductor Physics. A typical SIMS depth profile will indicate variations in the concentration of a dilute dopant or contaminant within a uniform optoelectronic material. The applications described below are "novel" in the sense that they focus on the major constituents of the material or they involve the use of special techniques to enhance depth resolution. Exam-

ples are drawn from SIMS studies at the author's institution, to the exclusion of numerous important and novel studies in the literature. The studies described below were, in each case, part of a broad experimental effort involving a number of principal investigators, as indicated in the references. The main conclusions of these studies are summarized.

In the "dynamic" SIMS technique, an ion beam is typically rastered over the sample surface, forming a square, flat-bottomed crater. Ions emerging from the central region of this crater are detected and individually tabulated according to their energy and mass. Count rates are recorded as a function of sputtering time, which may be converted to sputtering depth by subsequent measurement of the crater depth with a stylus profilometer. Oxygen or cesium bombardment are generally employed to dramatically enhance the yields of positive or negative ions, respectively. These en-

*Invited talk.

hancements are, to some extent, due to alteration of the surface work function. Ion yields, which determine sensitivity, vary by several orders of magnitude and are sensitive to the chemical environment from which the ions emerge. As a result, quantitation of SIMS profiles requires the use of standards and well controlled experiments. The most efficient SIMS studies involve comparison of many similar samples run under identical conditions. Numerous reviews of the SIMS technique are available^[1,2]. The reader is also referred to the proceedings of the biannual SIMS conference for discussions of diverse SIMS applications^[3].

This paper will describe four areas of study. In the first, a "backside SIMS" technique is employed to obtain high resolution depth profiles of the metal-semiconductor interface in III-V ohmic contacts. The technique is also applied to a study of low energy ion channeling in GaAs. The second area addresses diffusion and interdiffusion in semiconductor superlattices. These studies elucidated the mechanism of interdiffusion and also led to a refined theory of strained layer relaxation. Stoichiometry measurements in III-V semiconductors are briefly discussed. Applications include studies of Ga reevaporation and growth feedback during molecular beam epitaxy (MBE) of AlGaAs. The fourth topic polymer blend segregation and ordering, is also briefly addressed, and is currently the primary thrust of our SIMS laboratory.

II. Backside SIMS studies

The next generation of integrated III-V devices will require ohmic contacts which are shallow, non-spiking, uniform, bondable, thermally stable, and highly conductive. The palladium based non-alloyed contacts show special promise^[4]. Their abrupt metal-semiconductor interfaces also facilitate study by high resolution techniques such as SIMS. Resolution problems are encountered, however, when sputtering through the deposited metal layers. These layers may be non-uniform, may roughen when sputtered, and allow knock-in of metal constituents into the semiconductor. In the backside SIMS technique, the sample is thinned and then sputtered from the back (semiconductor) side so as to avoid these problems^[4,5].

The semiconductor samples are specially prepared by molecular beam epitaxy (MBE) or organo-metallic

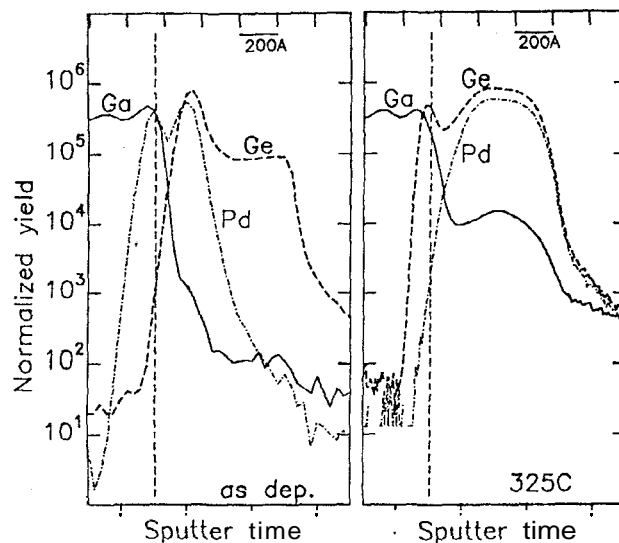


Figure 1: Backside SIMS depth profiles of a 130 nm Ge/60 nm Pd/GaAs ohmic contact, as-deposited (left) and annealed at 325°C for 30 minutes (right). The vertical dashed lines mark the position of the original GaAs surface. The Ge and Pd signals are much enhanced when reacted with each other or with GaAs. The Ga oscillation within the GaAs indicates one of the MBE marker layers. The Ge concentration drops by 4 orders of magnitude within ~ 10 nm of the interface in the annealed sample.

chemical vapor deposition (OMCVD) so that they contain an etch stop layer and several marker layers employed for subsequent alignment of profiles. The sample is first waxed onto a supporting semiconductor slab, and then mechanically thinned, using successively finer grades of grinding paper, to a thickness of $\sim 50 \mu\text{m}$. It is then immersed in an etching solution which removes the semiconductor substrate (GaAs or InP) but does not etch the thin (~ 50 nm) etch stop layer (AlGaAs or InGaAs). A second etchant selectively removes the etch stop layer. The entire process may be performed in less than half an hour per sample. Detailed procedures are presented elsewhere^[4-7]. The thinned ~ 300 nm structure typically contains four 10 nm thick ternary or quaternary layers spaced at 50 nm intervals. By aligning the marker layer profiles of various samples, the depth scales of each are well calibrated, and the relative motion of the metal-semiconductor interface with respect to the marker layers, due to semiconductor consumption and reaction, may be measured with a precision approaching 1 nm.

Fig. 1 illustrates two backside SIMS profiles of a Ge/Pd contact structure on GaAs, as deposited and

following a 30 minute 325°C anneal^[4,5]. The vertical dashed lines indicate the position of the original semiconductor surface as determined from alignment of the marker layers in these samples. The as-deposited sample consists of 130 nm of Ge on 60 nm Pd. Where the Ge and Pd react, the SIMS intensities are much enhanced, a so called SIMS "matrix effect". Following the anneal, which yields a highly conductive ohmic contact, the Ge concentration is observed to drop by 4 orders of magnitude within ~ 10 nm of the interface. Pure Ge has formed epitaxially between the semiconductor and the PdGe layer. Approximately 1 nm of GaAs has dissolved into the PdGe region, yielding the observed Ga profile. From combined SIMS and TEM studies, the sequence of events appears to be as follows: A thin ~ 6 nm Pd₄GaAs alloy layer is formed on deposition. When the PdGe reaction front reaches this alloy layer, it reclaims the Pd, leading to epitaxial regrowth of ~ 2 nm of GaAs. This 1 nm region is heavily doped with Ge ($> 10^{20}$ cm⁻³), sufficient to induce ohmic behavior.

Improved thermal and morphological properties were obtained with a Si/Pd contact where a thin Ge dopant spike was incorporated in the interfacial region^[6]. Subsequent SIMS studies of the Ge/Pd and Si/Pd contacts on InP have shown that regrowth of InP also occurs, however, the extent of interaction between Pd and InP is more difficult to control^[7].

Backside SIMS was also employed by Stoffel et al.^[8] to examine low energy Si implants in GaAs. These profiles of the Si³⁺ isotope (to avoid contaminant interference) showed surprisingly long channeling tails within the GaAs substrate. Such tails might be interpreted as a knock-in effect in frontside SIMS profiles. The results of this study indicated that ion channeling may degrade electrical and optical properties of devices exposed to low energy ion bombardment.

III. Superlattice interdiffusion studies

A heavily doped AlAs/GaAs superlattice annealed at temperatures above 600°C will eventually interdiffuse to form a uniform AlGaAs layer. The dependence of the rate of interdiffusion on doping and temperature is effectively studied by SIMS. SIMS can, of course, monitor the dopant concentration within the structure, but it is the high sensitivity to Al and Ga that proves especially beneficial in these studies. The superlattice

structure yields an oscillatory Al depth profile, as observed in Fig. 2^[9]. The peak-to-valley ratio of these oscillations is, a measure of the extent of interdiffusion. With a signal to noise ratio of $\sim 10^3$ for Al or Ga, SIMS can measure peak-to-valley ratios accurately over a wide range of values, and correlate these measurements to the Al diffusion coefficient. The figure shows an MBE structure with plateaus of Si doping, so that the dopant level at the center of each plateau remains constant during the anneal. 3 hour anneals at 700°C and 900°C are illustrated. Interdiffusion is clearly accelerated at the highest doping levels. Subsequent studies showed that at very high doping levels ($\sim 10^{20}$ cm⁻³) the Al diffusion coefficient is reduced. This effect is correlated with a reduction in electron concentration (dopant compensation). The Al diffusion coefficient was found, over a wide dopant range, to be proportional to the 3rd power of electron concentration, as is the concentration of the triply charged Ga vacancy^[10]. The results provide strong evidence for a vacancy mediated diffusion mechanism.

SIMS studies of Zn induced interdiffusion in InP/InGaAs superlattices revealed striking behavior. The In and Ga cations readily diffuse while As and P remain stationary. The result is a highly strained superlattice, free of grown-in defects^[11,12]. At high Zn concentrations, Zn completely displaces In in the InP layers to form Zn₃P₂. The results favor a cation kick-out mechanism for Zn induced interdiffusion. Transmission electron microscopy (TEM) of the interdiffused superlattices revealed numerous microtwin defects, oriented along the [111] direction and spanning the highly strained layers. Hwang, et al.^[11,12] demonstrated that these defects (partial dislocation pairs) are often the dominant mode of strained layer relaxation, as opposed to the conventional misfit dislocations treated in the theory of Matthews and Blakeslee.

IV. Stoichiometry measurement

The Al/Ga signal ratio measured in our quadrupole instrument was shown to be proportional to the true Al/Ga ratio over the entire (GaAs to AlAs) concentration range^[13]. While this result may seem trivial, it is generally not the case in the more common magnetic sector SIMS instruments, where a saturation of the Al/Ga intensity ratio occurs at high Al levels. The

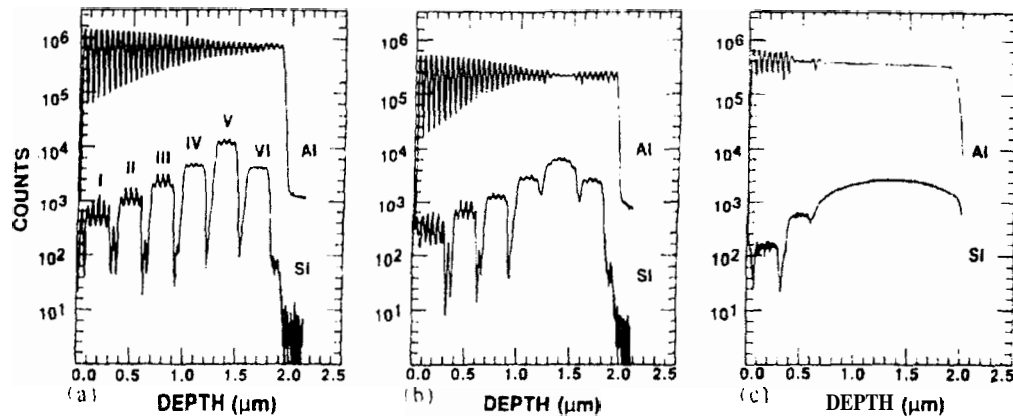


Figure 2: SIMS depth profiles of AlAs/GaAs superlattices as-grown (a) and annealed for 3 h at 700°C (b) and 900°C (c). Six Si dopant plateau regions are evident, with doping ranging from 2×10^{17} to $5 \times 10^{18} \text{ cm}^{-3}$ (AlH interference oscillations are visible in the Si profiles. The Al oscillations decay as the depth resolution is affected by sputtering depth.) Al-Ga interdiffusion is markedly accelerated at the highest doping levels.

ability to determine the sample stoichiometry, and to detect minute changes in stoichiometry, has been exploited in several studies.

In MBE growth of AlGaAs, Ga is known to escape from the growth surface at a temperature dependent rate which is quite appreciable at temperatures above 700°C. The escape of Ga may result from a temperature dependent sticking probability, or from Ga reevaporation which would in addition depend on the Ga surface concentration. Convincing results supporting both mechanisms have been published, and additional work is apparently required to determine the effect of various growth conditions on Ga loss. We examined a single MBE sample containing various alloy and superlattice regions grown at different temperatures^[13]. The results clearly showed that Ga loss in that sample was due to reevaporation and that the activation energy for reevaporation was 4.8 eV. SIMS allowed measurement of as little as 1% Ga loss.

Aspnes and coworkers^[14] have developed an optical method to monitor surface stoichiometry during MBE or OMCVD growth, thereby allowing feedback control of growth. Fig. 3 shows the composition profile of a 50 nm parabolic quantum well grown in this manner, as measured by SIMS. The distortions in the profile, such as the small peak at the 30 nm position, were found to be well correlated with the in-situ optical measurements.

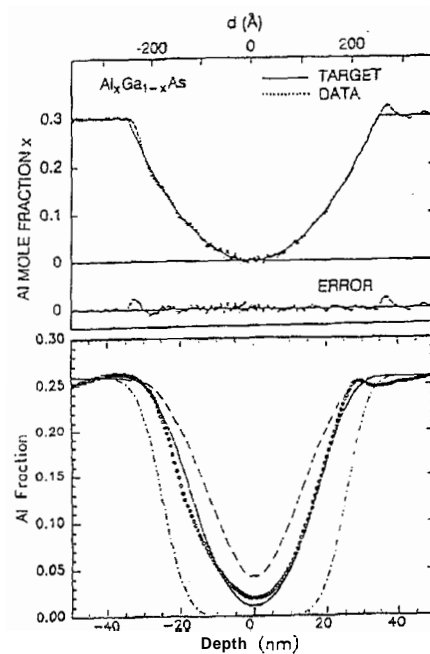


Figure 3: A 50 nm parabolic well grown by MBE under automated ellipsometer control. The SIMS data (lower) is well correlated with the in-situ ellipsometer data (upper dotted line). The SIMS data is well fit by a parabolic profile convolved with a 10 nm (FWHM) Gaussian function. This 10 nm value for the depth resolution was determined from an abrupt AlGaAs/GaAs interface deeper in the sample. Fits of 50 nm sawtooth (dashed) and square well (dash-dot) profiles are also shown.

V. Polymer studies

Polymer materials are increasingly employed in optoelectronics as optical transmission media, in active electrical devices, and of course in coating and structural applications. A technique to examine surface segregation, diffusion, and ordering in polymer blend films has recently been developed^[15]. A sacrificial polystyrene coating (–30 nm thick) is floated onto the sample of interest. This coating allows steady state sputtering conditions to be achieved prior to reaching the original sample surface, it protects the surface from contaminants, and it allows deposition of Au to avoid ion bombardment induced charging effects during the SIMS analysis. Argon bombardment is employed, to allow detection of oxygen and to avoid sensitivity variations associated with reactive ion sputtering at dissimilar interfaces. Deuterated polymers are incorporated into the blends to allow for sensitive detection of the motion of the blend components. Negative deuterium ions are detected, primarily to avoid an interference with H_2^+ . Oxygen, carbon, and chlorine are also more efficiently detected as negative ions. Nitrogen is undetectable as a monoatomic ion but is readily observed by monitoring the CN^- dimer ion. The depth resolution is –10 nm for 2 keV Argon bombardment at 30° off-normal incidence.

Fig. 4 illustrates preliminary data for the time dependence of triblock diffusion into polystyrene^[16]. The sample consisted of a 53 nm triblock copolymer film (polyvinyl pyridine (PVP) and deuterated polystyrene with polymerization index 124-552-124) on a 43 nm polystyrene layer on a Si substrate. The CN^- intensities, normalized to PVP volume fraction, are illustrated following 180°C anneals for 0, 20, 58, and 120 hours in vacuum. The nitrogen containing triblock ends initially segregate rapidly to the surface and the substrate interface. The triblock chains stretch out in a direction normal to these surfaces, and the PVP chain ends interact to form the ordered layer structure shown for the 120 hour anneal. The triblock chains at the surface loop around, with both ends located at a depth of –20 nm and the deuterated center segment exposed at the surface. The SIMS deuterium depth profiles are consistent with this description of ordering. A review of SIMS depth profiling studies of surface segre-

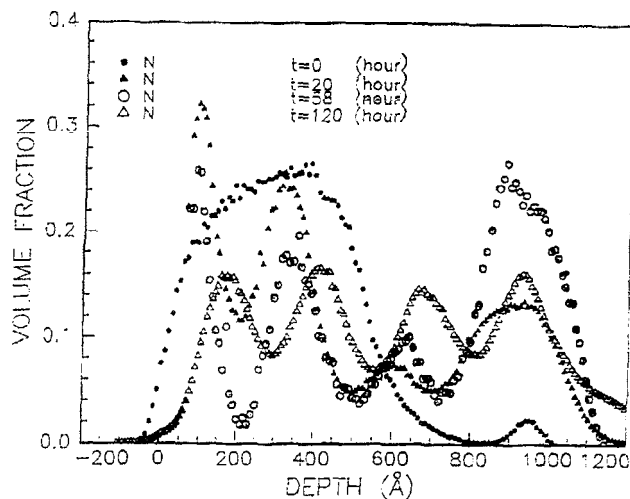


Figure 4: Time dependence of the diffusion of a 53 nm triblock layer into a 43 nm polystyrene layer on a silicon substrate, following anneals at 180°C of 0, 20, 58, and 120 hours. The CN^- SIMS depth profiles are shown, scaled to volume fraction. The triblock chains stretch, and the chain ends interact, to form the ordered four layer structure (at 120 h). The chain ends are attracted to the substrate interface and repelled from the surface.

gation in polystyrene blends, diffusion in cross-linked polystyrene, and grafting of end labeled polystyrene chains to an SiO_2 surface was recently published^[15].

VI. Conclusions

SIMS depth profiling studies of ohmic contact formation, low energy ion channeling, interdiffusion, and MBE growth effects in III-V structures have been described. The application of SIMS depth profiling to polymer blend structures was also briefly discussed. These SIMS studies are somewhat atypical, in that they do not emphasize detection of dilute species within a uniform semiconductor matrix. It is readily apparent that SIMS is an effective tool for fundamental studies of layer interactions, where high depth resolution and sensitivity to small concentration variations of the major constituents can be exploited.

References

1. A. Benninghoven, F. G. Rudenauer, and H. W. Werner, *Secondary Ion Mass Spectrometry - Basic Concepts, Instrumental Aspects, Applications, and Trends* (Wiley, New York, 1987).
2. S. A. Schwarz, *Secondary Ion Mass Spectrometry*, in the *Encyclopedia of Advanced Materials*, edited

- by D. Bloor, R. J. Brook, M. C. Flemings, and S. Mahajan, (Pergamon Press, Oxford) to be published.
3. A. Benninghoven, et al., ed's., *Secondary Ion Mass Spectrometry - SIMS VI*; 1990 SIMS VII; 1992 SIMS VIII (Wiley, New York, 1988).
 4. C. J. Palmstrom, S. A. Schwarz, E. Yablonovitch, J. P. Harbison, C. L. Schwartz, L. T. Florez, T. J. Gmitter, E. D. Marshall, and S. S. Lau, *J. Appl. Phys.* **67**, 334 (1990).
 5. S. A. Schwarz, C. J. Paknström, C. L. Schwartz, T. Sands, L. G. Shantharama, J. P. Harbison, L. T. Florez, E. D. Marshall, C. C. Han, S. S. Lau, L. H. Allen, and J. W. Mayer, *J. Vac. Sci. Tech.* **A8**, 2079 (1990).
 6. L. C. Wang, Y. Z. Li, M. Kappes, S. S. Lau, D. M. Hwang, S. A. Schwarz, and T. Sands, *J. Appl. Phys.* **71**, 3016 (1992).
 7. S. A. Schwarz, M. A. A. Pudensi, T. Sands, T. J. Gmitter, R. Bhat, M. Koza, L. C. Wang, and S. S. Lau, *Appl. Phys. Lett.* **60**, 1123 (1992).
 8. N. G. Stoffel, S. A. Schwarz, M. A. A. Pudensi, K. Kash, L. T. Florez, J. P. Harbison, and B. J. Wilkens *Appl. Phys. Lett.* **60**, 1603 (1992).
 9. P. Mei, H. W. Yoon, T. Venkatesan, S. A. Schwarz, and J. F. Harbison, *Appl. Phys. Lett.* **50**, 1823 (1987).
 10. S. A. Schwarz, T. Venkatesan, and P. Mei, *Mat. Res. Soc. Symp. Proc.* **126**, 43 (1988).
 11. D. M. Hwang, S. A. Schwarz, T. S. Ravi R. Bhat, and C. Y. Chen, *Phys. Rev. Lett.* **66**, 739 (1991).
 12. D. M. Hwang, S. A. Schwarz, R. Bhat, C. Y. Chen, and T. S. Ravi, *Opt. Quan. Electron.* **23**, S829 (1991).
 13. S. A. Schwarz, C. L. Schwartz, J. P. Harbison, and L. T. Florez, *Applications of $Al_xGa_{1-x}As$ Stoichiometry Measurement* by SIMS-VII, edited by A. Benninghoven, et al., (Wiley, New York, 1990), p. 467.
 14. W. E. Quinn, D. E. Aspnes, M. J. S. P. Brasil, M. A. A. Pudensi, S. A. Schwarz, M. C. Tamargo, S. Gregory, and R. E. Nahory, *J. Vac. Sci. Tech.* **B10**, 759 (1992).
 15. S. A. Schwarz, B. J. Wilkens, M. A. A. Pudensi, M. H. Rafailovich, J. Sokolov, X. Zhao, W. Zhao, S. Zheng, T. P. Russell, and R. A. L. Jones, *Molec. Phys.* **76**, 937 (1992).
 16. Y. Liu, W. Zhao, X. Zheng, A. King, A. Singh, M. H. Rafailovich, J. Sokolov, X. Zhao, K. H. Dai, E. J. Kramer, and S. A. Schwarz, *Bull. Amer. Phys. Soc.* **38-1**, 409 (1993).